

Insulin-Like Growth Factor Binding Protein-2 Is a Novel Therapeutic Target Associated with Breast Cancer

Alan I. So,^{1,3} Randy J. Levitt,⁴ Bernhard Eigl,¹ Ladan Fazli,¹ Motosugu Muramaki,¹ Sam Leung,² Maggie C.U. Cheang,² Torsten O. Nielsen,² Martin Gleave,^{1,3} and Michael Pollak⁴

Abstract Purpose: Insulin-like growth factor (IGF) binding proteins (IGFBP) modulate interactions of IGF ligands with the IGF-I receptor. The role of IGFBPs, and specifically IGFBP-2, in breast cancer progression has been poorly defined. This study assesses the effect of IGFBP-2 on the behavior of human breast cancer using clinical specimens as well as *in vitro* and *in vivo* experimental systems.

Experimental Design: 4,181 primary invasive breast cancers and 120 benign breast tissue samples were identified for tumor tissue microarray construction and immunostained with IGFBP-2 antibody. Estrogen receptor-negative MDA-MB-231 cells constitutively overexpressing IGFBP-2 (MDA-MB-231BP-2) were created to assess the effect of IGFBP-2 gain-of-function. MDA-MB-468 cells, naturally expressing IGFBP-2, were used to determine the effect of IGFBP-2 loss-of-function using OGX-225, an antisense oligonucleotide drug candidate.

Results: IGFBP-2 expression was significantly higher in breast cancer tissue compared with benign breast tissue. MDA-MB-231BP-2 cells grew more rapidly and were more resistant to paclitaxel both *in vitro* and *in vivo* compared with parental cells. OGX-225 decreased IGFBP-2 expression and attenuated the associated aggressive phenotype of MDA-MB-231BP-2 cells both *in vitro* and *in vivo*. Furthermore, OGX-225 inhibited the *in vitro* and *in vivo* growth of MDA-MB-468 cells.

Conclusions: This study provides evidence that IGFBP-2 expression is associated with breast cancer. Novel therapeutics targeting IGFBP-2, such as OGX-225, merit further evaluation.

The insulin-like growth factor (IGF) cell signaling pathway is implicated in the development and progression of many different malignancies (1). The IGF binding proteins (IGFBP) are a family of six proteins that bind with high affinity to IGF-I and IGF-II, thereby modulating the pro-survival and mitogenic effects of IGF. There is also evidence that IGFBPs have additional IGF-independent activity (2). IGFBP-2 is the second most abundant IGFBP in serum (3), and increased serum levels are associated with many tumors, including colon (4), ovarian (5), lung (6), and prostate (7) tumors. Furthermore, tissue IGFBP-2 expression has been correlated with tumor grade in

various tumors as well, including colon (8), adrenal (9), and mammary (10–12) tumors. Although the precise mechanism by which IGFBP-2 contributes to neoplastic behavior is incompletely defined, recent studies implicate relationships between IGFBP-2 expression and the activation of the phosphatidylinositol 3-kinase (PI3K)/Akt/mammalian target of rapamycin pathway (13, 14). However, the relationship of IGFBP-2 to breast cancer progression is not well described.

Breast cancer is a leading cause of cancer mortality of women. Unfortunately, many women with localized tumor will eventually develop metastatic disease. Management options for metastatic breast cancer include hormonal therapies as well as taxane-based chemotherapeutics or other cytotoxic agents. The 5-year survival rates of patients with metastases are <50% due to the limited benefit of current therapies and in turn the development of chemoresistant disease (15). However, <50% of these patients that fail first-line chemotherapy have a clinically useful response to traditional second-line chemotherapeutic agents (16).

Disease progression and metastatic spread of breast cancer result from stepwise genetic and epigenetic alterations of tumors and interactions with normal host cells. Understanding these molecular changes is crucial for identifying new targets and strategies that may delay time to tumor progression and improve survival.

Advances in the field of nucleic acid chemistry offer potential strategies to silence gene products mediating tumor progression and treatment resistance. Antisense oligonucleotide-based

Authors' Affiliations: ¹The Prostate Centre, Vancouver General Hospital; ²Genetic Pathology Evaluation Centre, British Columbia Cancer Agency; ³Department of Urological Sciences, University of British Columbia, Vancouver, British Columbia, Canada and ⁴Jewish General Hospital, McGill University, Montreal, Quebec, Canada

Received 2/14/08; revised 7/3/08; accepted 7/3/08.

Grant support: Terry Fox Foundation and National Cancer Institute of Canada (M. Gleave) and Canadian Breast Cancer Research Alliance "translational acceleration grant" (M. Pollak).

The costs of publication of this article were defrayed in part by the payment of page charges. This article must therefore be hereby marked *advertisement* in accordance with 18 U.S.C. Section 1734 solely to indicate this fact.

Note: Supplementary data for this article are available at Clinical Cancer Research Online (<http://clincancerres.aacrjournals.org/>).

Requests for reprints: Alan I. So, Department of Urological Sciences, University of British Columbia, 2733 Heather Street, Vancouver, British Columbia, Canada V5Z 3J5. Phone: 604-875-4818; Fax: 604-875-5654; E-mail: alan.so@ubc.ca.

©2008 American Association for Cancer Research.

doi:10.1158/1078-0432.CCR-08-0408

Translational Relevance

Breast cancer is a leading cause of cancer mortality of women; thus, development of novel therapeutics for this malignancy is essential. In this article, we provide preclinical proof of principle for the use OGX-225, an antisense oligonucleotide targeting IGFBP-2, as a candidate therapeutic for IGFBP-2-expressing breast cancers. Our results show that IGFBP-2 expression is more highly expressed in breast cancer than benign tissue and show a strong trend to adverse survival in hormone receptor-negative invasive breast cancer. Overexpression of IGFBP-2 in the MDA-MB-231 ER-negative breast cancer cell line conferred a growth advantage and chemoresistance. Correspondingly, down-regulation of IGFBP-2 using OGX-225, both in IGFBP-2-overexpressing MDA-MB-231BP-2 cells or in MDA-MB-468 cells that endogenously produces IGFBP-2, abrogates the cytoprotective benefits of IGFBP-2. Combined, these results contribute to the rationale for evaluating OGX-225 as a candidate therapeutic for IGFBP-2 expressing breast cancers.

agents specifically hybridize with complementary mRNA regions of a target gene to form RNA/DNA duplexes and thereby inhibit gene expression. Several antisense oligonucleotides targeted against specific genes involved in neoplastic progression have been evaluated as potential therapeutic agents (17). In fact, combined use of antisense oligonucleotide with other compounds, such as chemotherapeutic agents, has shown synergistic antineoplastic effects in several tumor models (18, 19). Generated using the 2'-O-(2-methoxy) ethyl backbone, OGX-225 (OncoGenex Technologies) is a second-generation antisense oligonucleotide that targets IGFBP-2 mRNA.

This study used a human breast cancer tissue microarray (TMA) series of >4,000 tumors to assess IGFBP-2 expression compared with a benign breast TMA. To further evaluate the significance of IGFBP-2 in breast cancer, we conducted functional analysis of IGFBP-2 using *in vitro* and *in vivo* models. These experiments identified a functional role for IGFBP-2 expression in promoting neoplastic growth, so we examined the effect of OGX-225 on the growth of IGFBP-2-expressing human breast cancer cells. We observed that this drug candidate potently suppressed IGFBP-2 levels and has both antiproliferative and chemosensitizing actions on breast cancer cells *in vitro* and *in vivo*.

Materials and Methods

TMA case series. The breast cancer TMA, known as the Breast Cancer Outcomes Unit (BCOU) TMA, was derived from a study cohort of 4,186 cases of invasive breast cancer diagnosed in the province of British Columbia in the period of 1986 to 1992 and has been fully described previously (20). The median follow-up time and age at diagnosis for this cohort was 12.4 and 60 years, respectively. All patients had been referred to the British Columbia Cancer Agency and had staging, pathology, treatment, and follow-up information maintained by the BCOU (21, 22). During the study era, ~75% of all breast cancer cases in British Columbia were referred to the British Columbia Cancer Agency. Nonreferred patients were generally elderly or treated by

mastectomy without indications for adjuvant therapy (21). The benign epithelial breast tissue array was composed of 120 samples obtained from patients without a diagnosis of breast cancer (Supplementary Table S1).

TMA immunostaining. TMAs were constructed by extracting 0.6-mm tissue cores obtained from areas of invasive carcinoma in formalin-fixed, paraffin-embedded archival tumor blocks using a Beecher microarrayer. Sections were deparaffinized and rehydrated through xylene and ethanol then transferred to 0.02% Triton for permeabilization. Slides in citrate buffer (pH 6) were heated in a steamer for 30 min. After cooling for 30 min and 3 × 5 min wash in PBS, the slides were incubated in 3% bovine serum albumin for 30 min. The slides were successively transferred to 3% H₂O₂ for 10 min and then incubated overnight with goat polyclonal anti-IGFBP-2 antibody (Santa Cruz Biotechnology) at the concentration of 1:200 in 1% bovine serum albumin. The next day, the primary antibody was washed extensively with PBS and the LSAB+ kit (DAKO) was used as the detection system. The Chromogen Nova-red (Vector Laboratories) was applied for 2 min and counterstaining was done with H&E (Vector Laboratories). After ethanol rehydration, a coverglass was applied with Cytoseal, a xylene-based mounting medium (Stephen Scientific). Stained TMA slides were digitally scanned on a BLISS Workstation (Bacus Laboratories). Estrogen receptor (ER) immunostaining and scoring using the SP-1 antibody is as described (20), as is progesterone receptor (clone 1E2; Ventana) and HER2 assessment by immunostaining and fluorescence *in situ* hybridization (23). Cases were considered hormone receptor positive if either estrogen or progesterone receptor was expressed in >1% of nuclei. IGFBP-2 immunostaining was determined as negative, weak, moderate, or strong based on a four-point visual score scheme, with "strong" being >50% of cells having cytoplasmic staining and "weak" being at least 5% of cells having cytoplasmic staining. Staining of IGFBP-2 was predominantly cytoplasmic. Kaplan-Meier plots and the log-rank test were used to evaluate survival differences.

Tumor cell lines. MDA-MB-231 and MDA-MB-468 cell lines were purchased from the American Type Culture Collection and cultured in DMEM (Invitrogen Life Technologies) and supplemented with 5% FCS.

Lentiviral infection of IGFBP-2 into MDA-MB-231 cells. The full-length cDNA for human IGFBP-2 was subcloned into the lentiviral vector pHR⁺-CMV-EGFP at the *Bam*HI and *Xho*I sites. Two vectors were created for study: pHR⁺-CMV-IGFBP-2 and pHR⁺-CMV (empty vector). Clone identity was verified using restriction digest analysis and plasmid DNA sequencing. Infectious lentivirus was generated by cotransfection of 1.5×10^6 293T cells with target plasmids with pCMVΔR8.2 (carries sequence necessary for viral assembly of lentivirus) and pMD.G, which expresses the vesicular stomatitis virus envelop glycoprotein G pseudotype as described previously (24). The 293T cells were transfected for 12 to 15 h, after which fresh medium was added for 24 h. After this, the virus-containing medium was collected and passed through a 0.45 μm filter. Early-passage MDA-MB-231 cells (passage 30) were plated on 10-cm plates, and competent retrovirus was added to 30 to 40 multiplicities of infection. The medium was changed after incubation for 16 h. The cells were passaged and harvested for UV microscopy to verify green fluorescent protein expression. Cell lysate were collected to ensure expression of IGFBP-2.

For *in vitro* growth assays, MDA-MB-231BP-2 and MDA-MB-231Mock (empty vector) were plated at 8×10^4 cells in six-well plates in DMEM with 5% fetal bovine serum (FBS). After 24 h, medium was changed to fresh DMEM with or without 5% serum. Cell viability was determined using 3-(4,5-dimethylthiazol-2-yl)-5-(3-carboxymethoxyphenyl)-2-(4-sulfophenyl)-2H-tetrazolium (MTS; Promega) proliferation assay described below on days 1, 3, 5, 6, and 10. MTS was combined with phenazine methosulfate (Sigma-Aldrich) in a ratio of 20:1 immediately before adding to cells. Mixture was then combined with medium in a 1:5 ratio and incubated at 1 h at 37°C in a humidified 5% CO₂ atmosphere. Medium was then aliquoted into 96-well plates and absorbance was read at 490 nm using a microplate reader (Becton Dickinson Labware). Each assay was done in triplicate.

Antisense oligonucleotides. 2'-O-(2-methoxy) ethyl-modified antisense oligonucleotides used in this study were synthesized as described previously (25). The sequence of IGFBP-2 antisense oligonucleotide (OGX-225; OncoGenex Technologies) was 5'-CAGCAGCCG-CAGCCCGCTC-3'. The control oligodeoxynucleotide sequence was 5'-CAGCAGCAGAGTATTTATCAT-3'.

Treatment of cells with antisense oligonucleotide. Oligofectamine (Invitrogen Life Technologies) was used to enhance transfection of cells. MDA-MB-231BP-2, MDA-MB-231Mock, and MDA-MB-468 cells (8×10^5) were treated with 50, 100, 250, or 500 nmol/L OGX-225 or scrambled control oligonucleotide (Scr-ODN) after preincubation for 20 min with 4 μ g/mL Oligofectamine in 5 mL serum-free Opti-MEM (Invitrogen). Four hours after starting the incubation, 2.5 mL DMEM/15% FCS was added to produce a final concentration of 5% FCS. Cells were treated once daily for 2 successive days and then harvested using 0.25% trypsin and lysed in radioimmunoprecipitation assay buffer plus protease inhibitors 72 to 120 h post-transfection for protein isolation. Complete protease inhibitor cocktail tablets from Roche were used according to the manufacturer's directions (one tablet for 50 mL extraction solution).

To determine the effect of OGX-225 on the viability of MDA-MB-231BP2, MDA-MB-231Mock, and MDA-MB-468 cell lines, 8×10^5 cells were treated with indicated concentration of OGX-225 or Scr-ODN in six-well plates. MTS assay as described above was done 72 h post-transfection to determine cell viability.

Western blot analysis. Cells were harvested by lysis in radioimmunoprecipitation assay buffer and protease inhibitors sheared with a 26-gauge needle. Protein (30 μ g) was separated by 10% PAGE, transferred to 0.45 μ m Immobilon-P Transfer membrane (Millipore), and analyzed by Western blotting with (1:400) goat IgG anti human IGFBP-2 (Santa Cruz Biotechnology). Loading levels were normalized using 1:2,000 anti-vinculin antibodies (Sigma) and densitometric analysis. To determine the amount of secreted IGFBP-2, conditioned medium obtained from cell lines cultured for 48 h in serum-free DMEM was used to perform Western blot analysis for IGFBP-2 as described above.

Immunofluorescence. MDA-MB-231BP-2 and MDA-MB-231Mock cells were grown on glass coverslips in DMEM plus 5% FBS for 48 h. Subsequently, cells were fixed with cold 3% acetone in methanol for 10 min at -20°C and permeabilized in 0.2% Triton in PBS. Slides were incubated in blocking solution 3% milk in PBS for 1 h and treated with primary mouse antibodies IGFBP-2 (Santa Cruz Biotechnology). Secondary fluorescent antibodies anti-mouse FITC were added for 1 h at room temperature with 3×5 min washes (0.1% Triton in PBS). Cells examined for localization of green fluorescent protein were mounted with fluorescent 4',6-diamidino-2-phenylindole Vectashield mounting medium (Vector). Images were captured using a Zeiss Axioplan II fluorescence microscope followed by analysis with imaging software (Northern Eclipse).

Chemotherapeutic agents. Paclitaxel was purchased from Biolyse Pharma. Stock solutions of paclitaxel were prepared with PBS to the required concentrations before each *in vitro* experiment. Dr. Helen M. Burt (Pharmaceutical Sciences, University of British Columbia) generously supplied polymeric micellar paclitaxel used for *in vivo* studies.

In vitro chemosensitization to paclitaxel using OGX-225. MDA-MB-231BP-2 and MDA-MB-231Mock cells were treated with 250 nmol/L OGX-225 or Scr-ODN in six-well plates as described above. After 48 h, cells were then treated with paclitaxel in a dose escalating fashion between 0 and 1,000 nmol/L for 24 h. MTS assays were done 48 h later as described above.

Flow cytometric analysis. Flow cytometric analysis of propidium iodide-stained nuclei was done as described previously (26). Briefly, MDA-MB-468, MDA-MB-231BP-2, and MDA-MB-231Mock cells were plated in 75 cm² dishes and treated as described above the following day. The cells were trypsinized 2 days after either OGX-225 or Scr-ODN treatment and analyzed for relative DNA content on a dual laser flow cytometer (Beckman Coulter Epics Elite; Beckman). Each assay was done in triplicate.

Effects of overexpression or OGX-225-induced knockdown of IGFBP-2 on MDA-MB-231BP-2 tumor growth in vivo. MDA-MB-231BP-2 or MDA-MB-468 cells (1×10^6) were inoculated s.c. with 0.1 mL Matrigel (Becton Dickinson Labware) in the flank region of 6- to 8-week-old female athymic nude mice (Harlan Sprague-Dawley) via a 27-gauge needle under halothane anesthesia. Tumor volume measurements were done once weekly and calculated by the formula: length \times width \times depth \times 0.5236 (27). Data points were expressed as average \pm SE tumor volume. Mice volumes were measured until week 7.

The effect of OGX-225 compared with Scr-ODN monotherapy on MDA-MB-231BP-2 tumor growth was evaluated in 20 mice bearing MDA-MB-231BP-2 tumors. OGX-225 or Scr-ODN (10 mg/kg) was injected i.p. once daily for 28 days and growth measured once a week (10 in each group). At the end of week 4, mice were sacrificed and tumors were harvested. Tumors were flash frozen in liquid nitrogen. Tumors were homogenized in radioimmunoprecipitation assay with proteinase inhibitor in a Dounce homogenizer. Western blot analysis was done on the total cell lysate to assess total IGFBP-2 levels within the xenografts. Protein (30 μ g) was separated by 10% PAGE, transferred to 0.45 μ m Immobilon-P Transfer membrane (Millipore), and analyzed by Western blotting with (1:400) goat anti-IGFBP-2 antibody (Santa Cruz Biotechnologies). Loading levels were normalized by blotting with (1:2,000) anti-vinculin (Sigma) for densitometric analysis.

To determine the effect of combined OGX-225 plus paclitaxel therapy on either MDA-MB-231BP-2 or MDA-MB-231Mock xenografts, similarly inoculated mice as described above were randomly selected for treatment with paclitaxel plus OGX-225 or Scr-ODN when MDA-MB-231BP-2 or MDA-MB-231Mock tumors reached 1,000 mm³. All randomization was done by an animal technician in a blinded fashion. Each experimental group consisted of 10 mice. After randomization, 10 mg/kg OGX-225 or Scr-ODN was injected i.p. once daily for 42 days. Paclitaxel (0.5 mg) was administered i.v. three times weekly from days 7 to 14 and days 21 to 28. All animal procedures were done according to the guidelines of the Canadian Council on Animal Care and with appropriate institutional certification. Mice tumors were harvested on day 28, and half of each tumor was formalin-fixed and paraffin-embedded or flash-frozen in liquid nitrogen and then treated with radioimmunoprecipitation assay buffer to obtain total cell lysate.

To determine the effect of OGX-225 treatment on apoptotic rates in tumors, TUNEL staining (Apoptosis Detection Kit from Chemicon) was done on representative samples of xenografts treated with combination therapy.

The effect of OGX-225 monotherapy on MDA-MB-468 tumor growth was done by randomly selecting 6 mice to receive OGX-225 and 6 mice to receive Scr-ODN using same treatment schedule as above. All mice were then inoculated with MDA-MB-468 as described above. Tumor take rates and tumor volumes were recorded once weekly.

Statistical analysis. Results were expressed as mean \pm SE. Statistical analysis was done by an unpaired two-tailed *t* test (GraphPad Instat 3) or χ^2 test. $P \leq 0.05$ was considered significant. Nonparametric Spearman correlation and Kendall τ -b test analyses were carried out to identify potential correlations between IGFBP-2 expression and other known prognostic factors. Because multiple subset analyses were run on the training set, apparently significant correlations were put forward at a meeting of the BCOU for specific testing on the validation set, with Bonferroni correction for significance. The validation set analysis was prespecified to use an IGFBP-2 cut point between weak and moderate (score 0, 1 versus score 2, 3) and was done by a separate researcher (M.C.) who was not involved in the training set data analysis. As training and validation set results were not significantly different, the final data set was aggregated.

Results

IGFBP-2 expression in TMA. Supplementary Table S1 shows the diagnoses of epithelial tissue used in the benign tissue TMA. Figure 1A shows the frequency and intensity of IGFBP-2

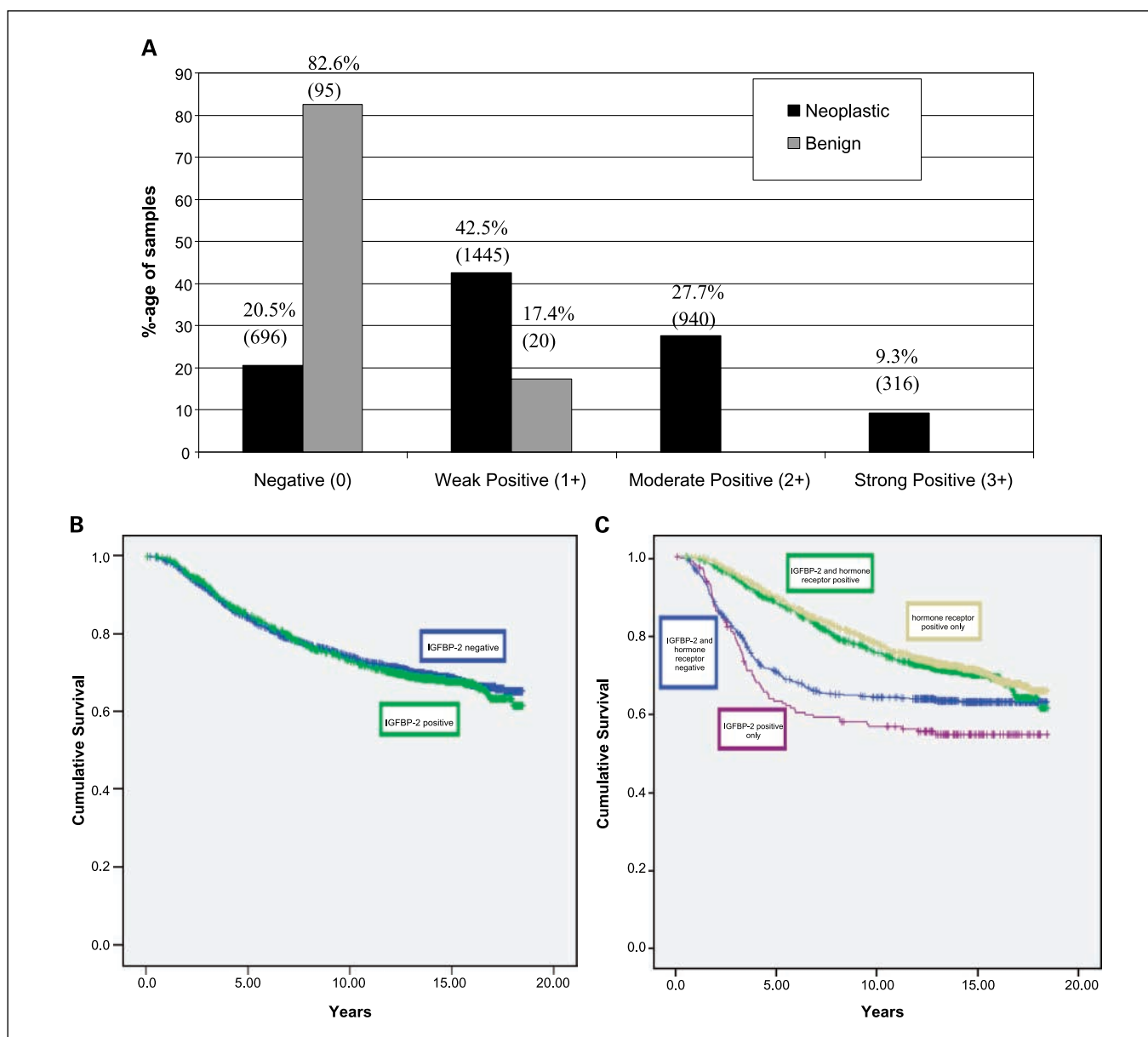


Fig. 1. Expression of IGFBP-2 in breast tissue TMA. **A**, summary of expression intensity in both BCOU TMA and benign breast TMA. Staining was validated by multiple control slides by omitting the primary antibody. **B**, breast cancer death-specific survival based on IGFBP-2 expression. *Blue line*, cases with IGFBP-2 negative or weak expression; *green line*, cases with IGFBP-2 moderate or strong expression. No prognostic significance was observed between tumors with negative/weak and moderate/strong IGFBP-2 expression ($P = 0.64$, log rank). **C**, breast cancer death-specific survival based on IGFBP-2 and hormone receptor expression. *Gold line*, cases with hormone receptor-positive and IGFBP-2 negative/weak expression; *green line*, cases with hormone receptor-positive and IGFBP-2 moderate/strong expression; *blue line*, cases with hormone receptor-negative and IGFBP-2 negative/weak expression; *purple line*, cases with hormone receptor-negative and IGFBP-2 moderate/strong expression. Among the subset with positive hormone receptor expression, IGFBP-2 expression was not prognostic ($P = 0.78$, log rank), whereas among tumors with negative hormone receptor expression, IGFBP-2 was associated with a trend to worse breast cancer disease-specific survival ($P = 0.068$, log rank).

expression in both the BCOU breast cancer and the benign breast TMA. IGFBP-2 expression was detected in significantly more cases in the BCOU TMA (82.6%) compared with the benign tissue TMA (17.4%; $P < 0.001$, χ^2 test). In the benign breast tissue array, any detected staining for IGFBP-2 was only weakly positive.

IGFBP-2 expression in both TMAs, when present, was predominantly cytoplasmic (Supplementary Fig. S1A). Missing cores were found in both TMAs (16.2% of cores in the BCOU TMA and 5.0% of cores in the benign tissue TMA) and may be due to either missing tissue on the slide, fold artifact, or insufficient cancer (<50 cells) in a core.

IGFBP-2 correlation with clinical markers and patient outcome. In the series as a whole, no prognostic significance was observed between tumors with negative/weak and moderate/strong IGFBP-2 expression (Fig. 1B; $P = 0.64$, log rank). In clinical practice, breast cancer patients are stratified by estrogen and progesterone hormone receptor and HER-2 status. Within the BCOU TMA, 3,117 tumors were assessable for both IGFBP-2 and hormone receptors. 2,350 (75.4%) tumors had positive hormone receptor expression, whereas 767 (24.6%) tumors had negative hormone receptor expression. A statistically significant positive correlation (Kendall's τ -b correlation

coefficient = 0.165, $P < 0.001$) between IGFBP-2 expression and hormone receptor expression status was found. Expression of IGFBP-2 relative to hormone receptor status is shown in Supplementary Table S2. Among the subset with positive hormone receptor expression, IGFBP-2 expression was not prognostic ($P = 0.78$, log rank), whereas among tumors with negative hormone receptor expression, IGFBP-2 was associated with a trend to worse breast cancer disease-specific survival (Fig. 1C; $P = 0.068$, log rank). IGFBP-2 expression was also compared with HER-2 expression and no significant correlation was observed (Kendall's τ -b = 0.005, $P = 0.792$).

Overexpression of IGFBP-2 in MDA-MB-231 cell line. Figure 2A confirms high IGFBP-2 protein levels within MDA-MB-231 cells stably expressing human IGFBP-2 cDNA (MDA-MB-231BP-2). MDA-MB-231BP-2 and empty-vector controls (MDA-MB-231Mock) were cultured in serum-free DMEM, and Western blots done on 48 h conditioned medium show that the MDA-MB-231BP-2 cell line also secretes significant amounts of IGFBP-2 (Fig. 2B). Immunofluorescence further confirms increased intracellular IGFBP-2 levels in the MDA-MB-231BP-2 cell line (Fig. 2C). MDA-MB-231 cells had low expression levels of IGFBP-2 similar to that of MDA-MB-231Mock cells (data not shown).

In vitro and in vivo effects of IGFBP-2 overexpression. MDA-MB-231BP-2 cells, compared with Mock-lentivirus-infected cells, begin to show significant growth advantages after 5 days of growth in DMEM with 5% FBS. Differences in cell growth continue increasing up to day 10 (Fig. 3A). Similar results were observed when cell lines were cultured in serum-free medium (Fig. 3B). Although both cell lines begin to have reduced cell viability on day 5, MDA-MB-231BP-2 cells remain more resistant to the effects of serum starvation.

We next compared the rate of tumor growth of MDA-MB-231BP-2 ($n = 10$) cells *in vivo* to MDA-MB-231Mock cells ($n = 10$). Beginning week 3 after tumor cell injection, average tumor volume increased more rapidly in MDA-MB-231BP-2 tumors compared with Mock-lentivirus-infected controls (Fig. 3C). At the time of sacrifice, tumor volume was double in MDA-MB-231BP-2 relative to MDA-MB-231Mock cells.

Effect of OGX-225-induced IGFBP-2 knockdown on cell viability and chemosensitization in vitro. Treatment of MDA-MB-231BP-2 cell lines with OGX-225 significantly decreases IGFBP-2 expression in a dose-dependent and sequence-specific manner (Fig. 4A). Transfection of cells with OGX-225 causes reduced cell viability in MDA-MB-231BP-2 cells in a dose-dependent fashion but not in MDA-MB-231Mock cells (Fig. 4B). No effect in cell viability of Scr-ODN on either cell line was observed. Interestingly, when we decrease IGFBP-2 levels in MDA-MB-231BP-2 cells with OGX-225, the resultant cell viability is less than that of MDA-MB-231Mock treated with either Scr-ODN or OGX-225. Flow cytometric analysis of MDA-MB-231BP-2 cells 2 days after treatment with 100 nmol/L OGX-225 or Scr-ODN revealed that the fraction of MDA-MB-231BP-2 cells undergoing apoptosis (sub-G₀-G₁ fraction) was 3-fold higher in cells treated with OGX-225 when compared with Scr-ODN (data not shown). MDA-MB-231Mock cells treated with OGX-225 experienced a modest 1.5-fold increase in apoptosis compared with cells treated with Scr-ODN. This suggests that cells overproducing IGFBP-2 become dependent on cell signaling pathways that are stimulated by IGFBP-2 and that the growth suppression after OGX-225 treatment in the MDA-MB-231BP-2 cells reflects an increased apoptotic rate. To determine if IGFBP-2 influences the sensitivity of MDA-MB-231 cells to the cytotoxic drug paclitaxel, MDA-MB-231Mock and MDA-MB-231BP-2 xenografts were treated with OGX-225 or Scr-ODN in combination with increasing doses of paclitaxel. As seen in Fig. 4C, MDA-MB-231BP-2 cells are more resistant to paclitaxel-induced growth inhibition than MDA-MB-231Mock cells (comparing Scr-ODN-treated groups). However, the addition of OGX-225 to paclitaxel treatment of the MDA-MB-231BP-2 cell line chemosensitizes the cells, resulting in cell viabilities less than MDA-MB-231Mock cells treated with paclitaxel. This once again is consistent with the view that the MDA-MB-231BP-2 cells become more dependent on IGFBP-2-stimulated pathways.

Effect of OGX-225 monotherapy in vivo. Inhibition of MDA-MB-231BP-2 xenograft growth was observed when animals were treated with OGX-225 compared with Scr-ODN (Fig. 5A).

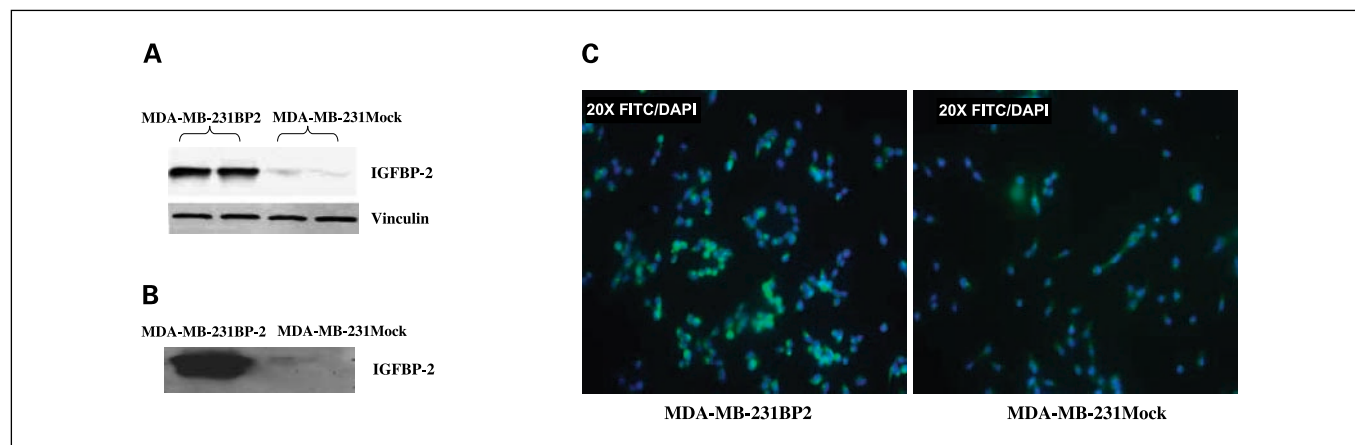
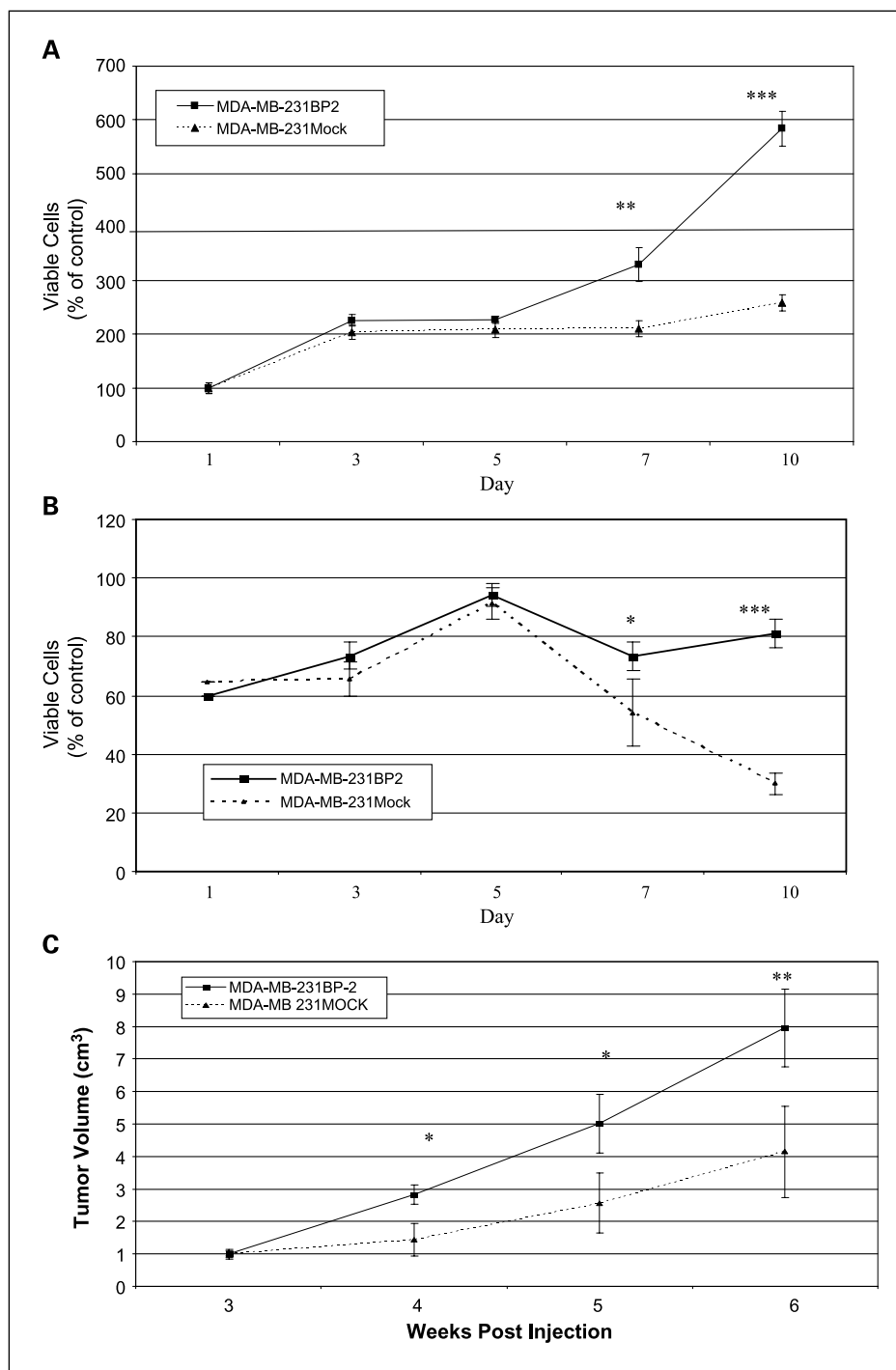


Fig. 2. Creation of IGFBP-2-overexpressing breast cancer cell line. *A*, expression of IGFBP-2 in MDA-MB-231 lentivirus-infected cells. Western blot showing protein expression of IGFBP-2 of total cell lysate in MDA-MB-231 cell lines infected with IGFBP-2 lentivirus compared with Mock controls. *B*, IGFBP-2 expression in conditioned medium, normalized to cell number. Western blot for IGFBP-2 was done on medium obtained from cultured cells incubated at 37°C over 48 h. *C*, immunofluorescence of IGFBP-2-stained cells. Cell lines were immunostained for IGFBP-2 with fluorescently-tagged secondary antibodies. MDA-MB-231BP-2 cell lines produced increased amounts of intracellular IGFBP-2 compared with MDA-MB-231Mock control.

Fig. 3. Growth of MDA-MB-231BP-2 and MDA-MB-231Mock. *A*, *in vitro* DMEM with 5% FBS. *B*, *in vitro* DMEM without FBS. *C*, *in vivo* in nude female mice. *A*, cells were plated at 70% confluency and then incubated at 37°C from 1 to 10 d. On days 1, 3, 5, 7, and 10, MTS assay was done to assess for changes in cellular growth. Cell viability is a ratio of the number of cells at each time point relative to that at day 1 for each group. *B*, cells were plated at 70% confluency and then incubated at 37°C in 5% FBS. After 24 h, medium was replaced without FBS. Cell viability is a ratio of the number of cells at each time point relative to that at day 1 of plates with 5% FBS. *A* and *B*, medium was not changed after day 1. *C*, two groups of 10 female athymic mice were injected with 10^6 cells: one group with MDA-MB-231BP-2 and the other with MDA-MB-31Mock. Tumor volume measurements were done once weekly over a 7-wk period. *, $P \leq 0.05$ was considered significant; **, $P \leq 0.01$; ***, $P \leq 0.001$.



Tumor take was 100% in each group, but mice receiving the Scr-ODN developed larger and more rapidly growing tumors than those receiving OGX-225. Tumors were excised at the time of sacrifice and IGFBP-2 protein levels were determined by Western blotting (Fig. 5B; Supplementary Fig. S2). Significantly decreased IGFBP-2 protein levels were detected in MDA-MB-231BP-2 xenografts excised from OGX-225-treated mice, showing that OGX-225 can reduce the expression of its target *in vivo*.

Effect of OGX-225 and paclitaxel cotreatment in vivo. To determine the effect of combination therapy using paclitaxel

and OGX-225, MDA-MB-231BP2 and MDA-MB-231Mock xenografts were treated with paclitaxel and either OGX-225 or Scr-ODN (Fig. 5C). All treatment groups, except MDA-MB-231BP2 tumor-bearing mice treated with paclitaxel plus Scr-ODN, responded to therapy at weeks 1 and 3. MDA-MB-231BP2 tumors treated with Scr-ODN grew more rapidly than MDA-MB-231BP2 xenografts treated with OGX-225, suggesting a chemosensitizing effect of the OGX-225. MDA-MB-231Mock xenografts responded to chemotherapy with durable suppression of tumor growth in mice treated with either OGX-225 or Scr-ODN. Interestingly, *in vivo* growth of the OGX-225-treated

MDA-MB-231BP-2 cells was similar to the growth of Scr-ODN-treated MDA-MB-231Mock cells. TUNEL assay was done on all tumors to determine whether apoptotic rates may contribute to the growth differences in combination therapy regimens (Supplementary Fig. S3). MDA-MB-231BP-2 xenografts treated with both OGX-225 and paclitaxel had higher TUNEL immunostaining compared with similar xenografts treated with Scr-ODN and paclitaxel ($P = 0.04$, χ^2 analysis).

Down-regulation of IGFBP-2 in MDA-MB-468 cells treated with OGX-225. Having shown that MDA-MB-231BP-2 cells were growth inhibited by OGX-225 *in vitro* and *in vivo*, we wished to determine the effect of this drug candidate on MDA-

MB-468 breast cancer cell line that endogenously express high levels of IGFBP-2. OGX-225 resulted in a dose-dependent and sequence-specific knockdown of IGFBP-2 in MDA-MB-468 cells (Fig. 6A). OGX-225 treatment also resulted in characteristic morphologic changes, suggesting increased apoptosis, including reduced cell concentration, cellular rounding, and membrane blebbing (Fig. 6B). Consistent with our results with the MDA-MB-231BP-2 cells, OGX-225 treatments inhibited MDA-MB-468 cell growth *in vitro* compared with Scr-ODN (Fig. 6C). Furthermore, flow cytometric analysis of MDA-MB-468 cells 2 days after treatment with 100 nmol/L OGX-225 had a significantly higher sub-G₀-G₁ fraction of cells compared with

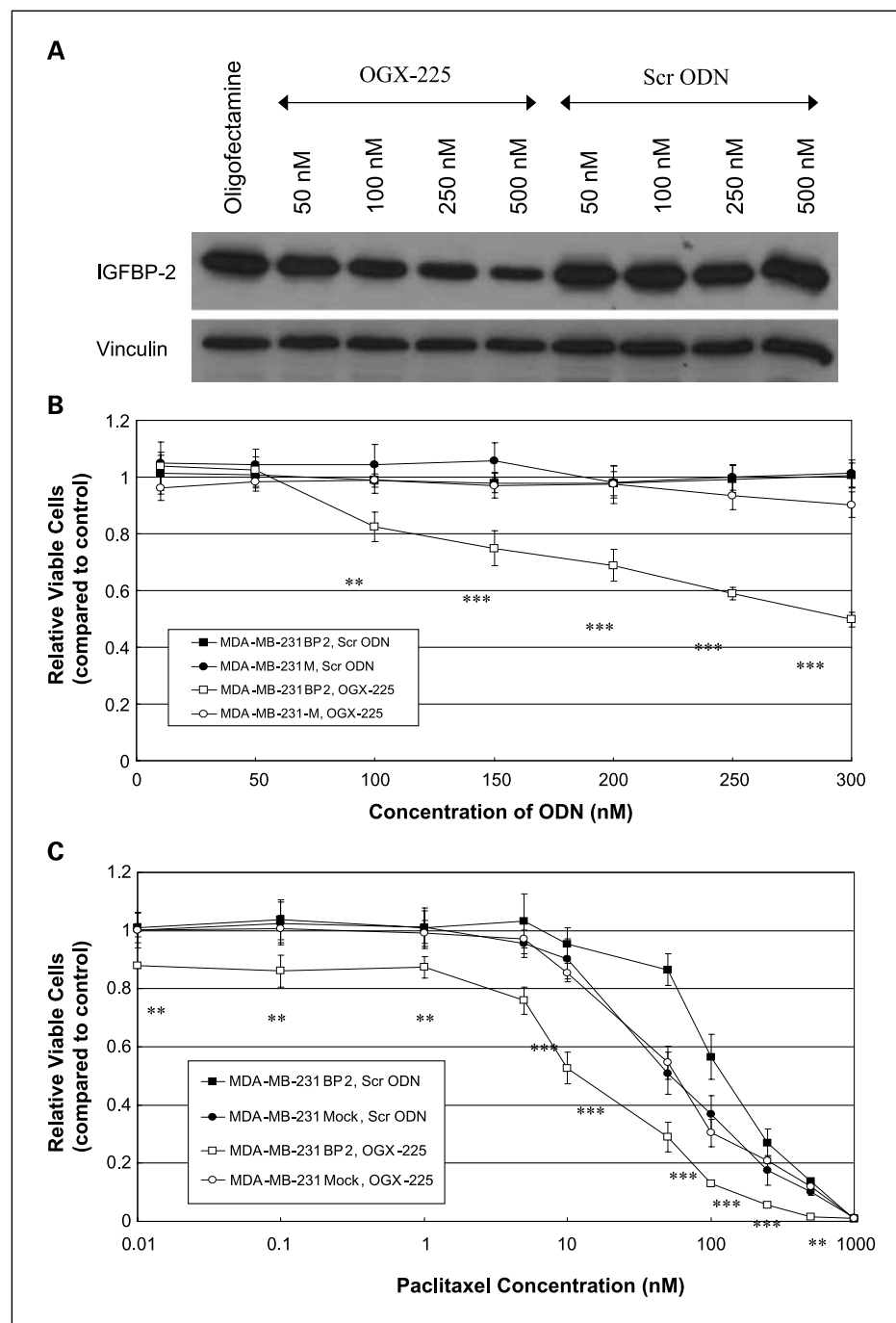
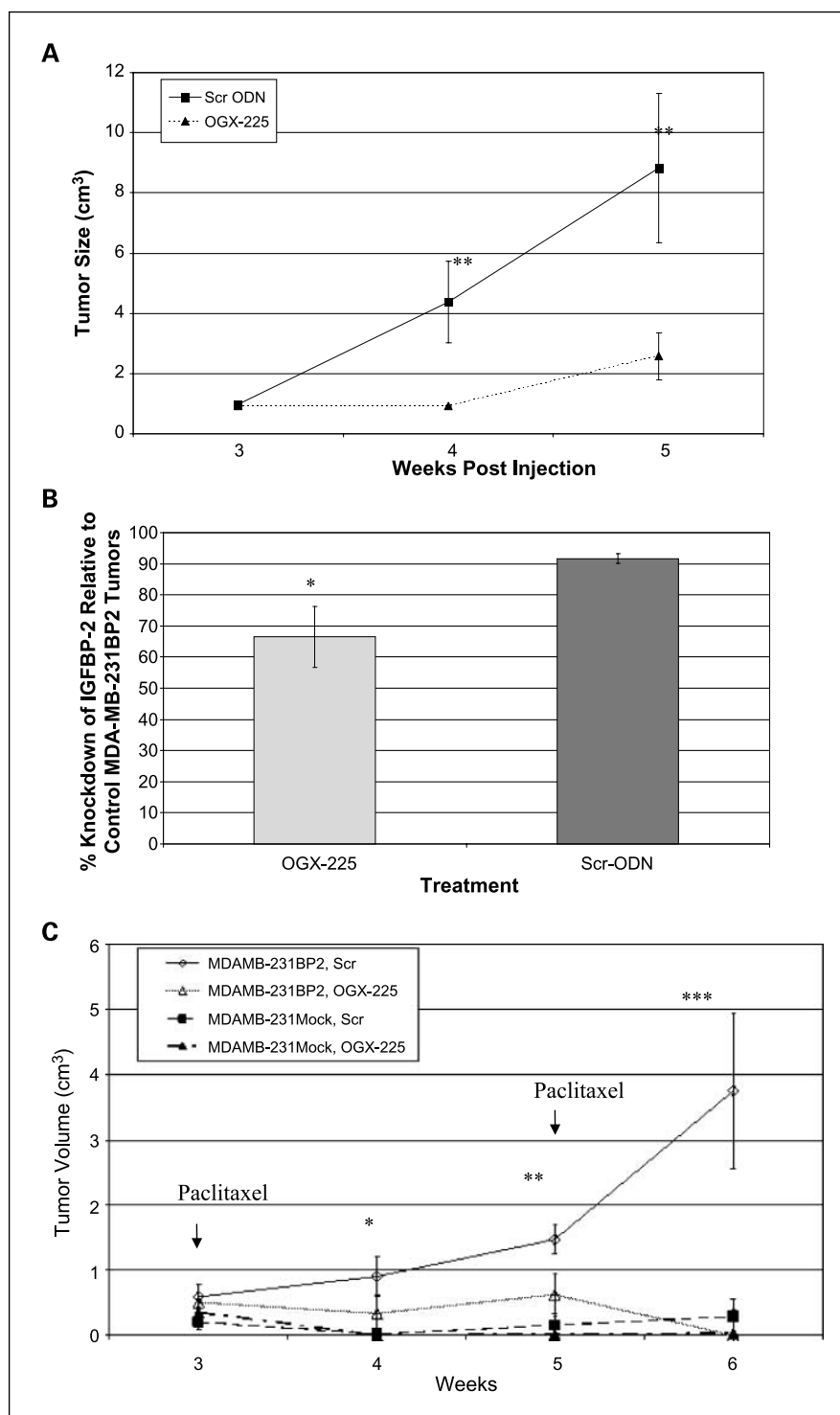


Fig. 4. Effect of OGX-225 treatment on MDA-MB-231BP-2 cells *in vitro*. **A**, dose-dependent and sequence-specific inhibition of IGFBP-2 by OGX-225 treatment on MDA-MB-231BP2 cells. MDA-MB-231BP-2 cells were treated with 50, 100, 250, or 500 nmol/L OGX-225 or Scr-ODN (two treatments on successive days) for 4 h at 37°C. OGX-225 or Scr-ODN-treated cells were harvested for total cell lysate on day 5 post transfection and 30 µg protein was analyzed by Western blot. Loading levels were normalized by blotting with anti-vinculin antibody. "Oligofectamine" refers to Oligofectamine-only control. **B**, dose-dependent inhibition of growth in MDA-MB-231BP-2 cells. MDA-MB-231BP-2/MDA-MB-231Mock cells were treated with six dose-escalating doses of OGX-225 or Scr-ODN between 0 and 300 nmol/L (two treatments on successive days) for 4 h at 37°C. MTS assay was done on cell lines 72 h after initial transfection. Cell viability at each concentration is relative to cell growth of cells when given no oligonucleotide (control). **C**, chemosensitization of MDA-MB-231BP-2 to paclitaxel after treatment with OGX-225. MDA-MB-231BP-2/MDA-MB-231Mock cells were treated with 250 nmol/L OGX-225 or Scr-ODN for 4 h at 37°C. Paclitaxel was added 48 h after transfection and incubated for 48 h, after which a MTS assay was done. Cell viability at each concentration of paclitaxel is relative to cell growth of cells when given no paclitaxel or oligonucleotide (control). *, $P \leq 0.05$ was considered significant; **, $P \leq 0.01$; ***, $P \leq 0.001$.

Fig. 5. Effect of OGX-225 treatment on MDA-MB-231BP-2 cells *in vivo*. **A**, *in vivo* effect of single-agent therapy of OGX-225 or Scr-ODN in MDA-MB-231BP2 xenografts. Twenty athymic mice injected with MDA-MB-231BP2 were randomly selected to receive either OGX-225 or Scr-ODN over a 4-wk period once tumors became >1 mL. **B**, down-regulation of IGFBP-2 in xenografts treated with OGX-225 versus Scr-ODN monotherapy. Mean expression of IGFBP-2 in the two groups relative to untreated controls. Mice treated with OGX-225 had significantly higher suppression of IGFBP-2 in MDA-MB-231BP2 tumors compared with those treated with Scr-ODN. Xenografts with no treatment were used as control. **C**, OGX-225 enhances paclitaxel activity in MDA-MB-231BP2 xenografts *in vivo*. Female athymic mice were injected with 10^6 cells. When tumors reached $1,000$ mm³, usually 3 to 4 wk after injection, 20 mice were randomly selected for treatment with 10 mg OGX-225 or scrambled controls once daily by i.p. injection for 42 d. Paclitaxel (0.5 mg) was administered i.v. three times a week from days 7 to 14 and from days 21 to 28 in all groups. Tumor volume measurements were done once weekly. *, $P \leq 0.05$ was considered significant; **, $P \leq 0.01$; ***, $P \leq 0.001$.



cells treated with Scr-ODN (70.9% compared with 39.9%, $P < 0.01$), suggesting that OGX-225 treatment increased the rate apoptosis (data not shown).

In vivo study of the effect of OGX-225 administration in mice injected with MDA-MB-468 cells revealed that OGX-225-treated mice had significantly reduced tumor take rate (17% versus 100%) and growth compared with those that received Scr-ODN (Fig. 6D), providing further evidence for a role for IGFBP-2 in the progression of these xenografts.

Discussion

Recent immunohistochemical studies are consistent with the hypothesis that IGFBP-2 expression increases with breast cancer progression from hyperplasia through atypical hyperplasia and carcinoma *in situ* to invasive carcinoma, linking IGFBP-2 to tumor progression (10–12, 28, 29). Our results, using a much larger cohort of breast cancer patients, confirm the association of increased expression of IGFBP-2 with transformation of

breast epithelial cells. High IGFBP-2 staining has been associated with poor prognosis in other tumors, including glioblastoma (30), bladder (31), childhood acute lymphoblastic leukemia (32), and prostate cancer (33). Although our results with >4,000 cases show that IGFBP-2 expression was not prognostic in the cohort as a whole, it did show a strong trend to adverse survival among patients with hormone receptor-negative invasive breast cancer.

Furthermore, we identify, for the first time using TMA analysis, a correlation between ER status and IGFBP-2, confirming previous reports from *in vitro* studies with various breast cancer cell lines showing a relationship between ER status and IGFBP-2 expression (34, 35). ER-positive cell lines have been shown to have increased expression of IGFBP-2 compared with ER-negative cell lines; accordingly, ER expression in breast cancer has correlated with IGFBP-2 in our TMA analysis (34, 35). However, in these patients, IGFBP-2 did not correlate with adverse outcome.

Recent evidence suggests that IGFBP-2 may be involved in the transformation from estrogen dependence to a phenotype that

is resistant to antiestrogens (36). Interestingly, Helle et al. (37) reported that elevated serum levels of IGFBP-2 was associated with a worse disease-specific survival in a cohort of female breast cancer patients with metastatic or locally recurring breast cancer treated with tamoxifen; in contrast, serum IGFBP-2 lacks prognostic or predictive power in postmenopausal women (38). These results confirm recent *in vitro* data that suggest IGFBP-2 expression may be negatively regulated by estrogens and, more importantly, that IGFBP-2 is overexpressed in breast cancer cells resistant to antiestrogen therapy (36). Fog et al, reported that breast cancer cells resistant to the antiestrogen RU 58,688 have baseline IGFBP-2 levels that are significantly higher compared with parental cells; furthermore, these levels increase in a dose-dependent fashion after the administration of RU 58,688 (36).

In prostate cancer, several reports similarly indicate that IGFBP-2 levels are repressed by androgen (39). IGFBP-2 expression increases after androgen ablation and functions to promote progression by suppressing apoptosis and enhancing growth under androgen-deprived conditions (40). Collectively,

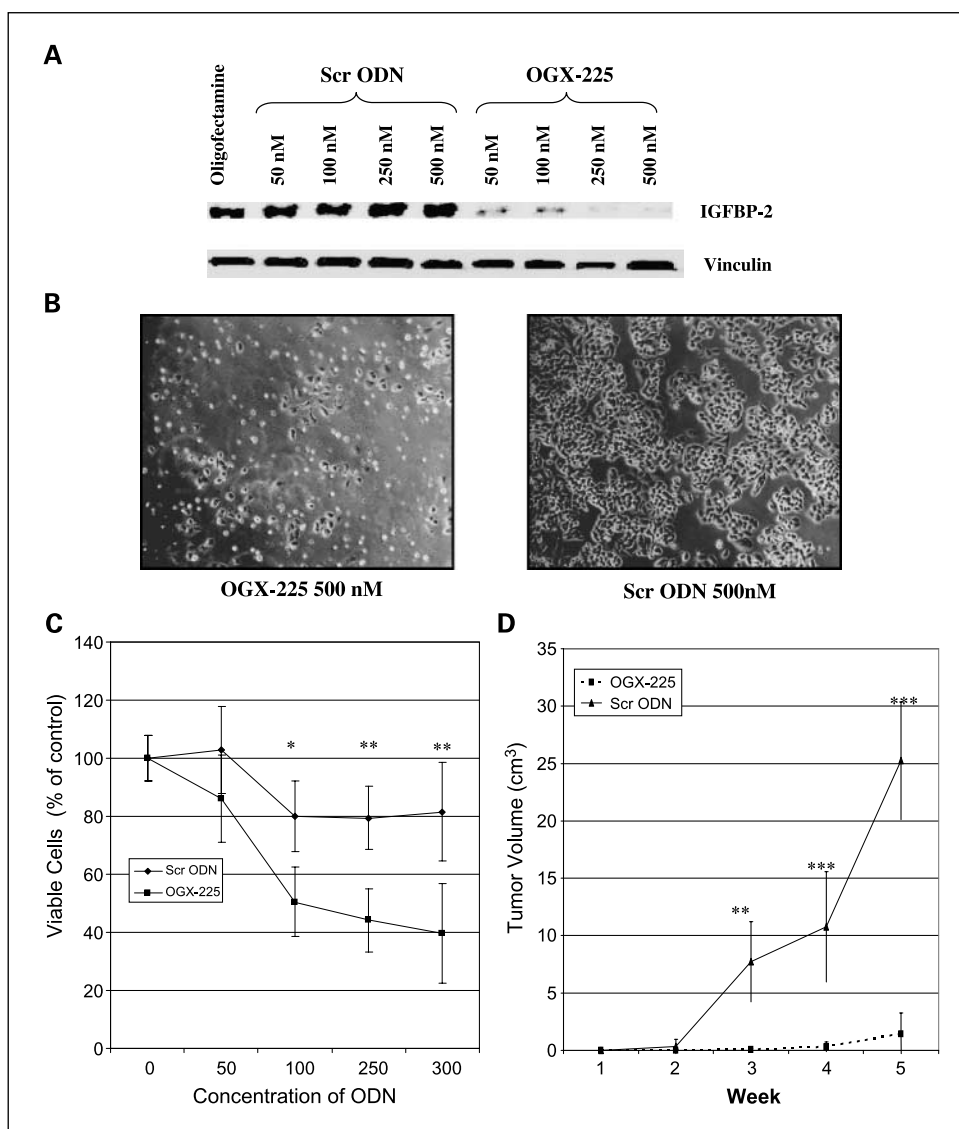


Fig. 6. Effect of OGX-225 treated in MDA-MB-468 cell line. **A**, dose-dependent sequence-specific down-regulation of IGFBP-2 in MDA-MB-468 cell line transfected with OGX-225. MDA-MB-468 cells were treated with 50, 100, 250, or 500 nmol/L OGX-225 or Scr-ODN (two treatments on successive days) for 4 h at 37°C. OGX-225 or Scr-ODN-treated cells were harvested for total cell lysate on day 5 post-transfection and 30 µg protein was analyzed by Western blot. Loading levels were normalized by blotting with anti-vinculin antibody. **B**, *in vitro* effect of OGX-225 treatment in MDA-MB-468 cell line. ×40 magnification of the effect of OGX-225 *in vitro* on MDA-MB-468 cell line, including reduced cell concentration, rounding of cells, cytoplasm shrinkage, and membrane blebbing. **C**, dose-dependent inhibition of *in vitro* growth. MDA-MB-468 cells were treated with six dose-escalating concentrations of OGX-225 or Scr-ODN between 0 and 300 nmol/L (two treatments on successive days) for 4 h at 37°C. MTS assay was done on cell lines 72 h after initial transfection. **D**, tumor growth rates of MDA-MB-468 xenografts treated with OGX-225. Twelve female athymic mice were injected with 10⁶ cells. Starting 1 wk before tumor inoculation, 6 mice were randomly selected for treatment with 10 mg OGX-225 or scrambled controls once daily by i.p. injection for 42 d. Tumor volumes rates were measured weekly. *, *P* ≤ 0.05 was considered significant; **, *P* ≤ 0.01; ***, *P* ≤ 0.001.

these experimental and TMA biomarker studies indicate that high levels of IGFBP-2 function to confer a growth advantage and a worse prognosis mainly in ER-negative tumors and suggest that deregulated IGFBP-2 expression may be a key component of survival after hormone therapies.

We evaluated the effect of overexpression of IGFBP-2 in an ER-negative breast cancer cell line, MDA-MB-231, which does not normally express IGFBP-2. Overexpression of IGFBP-2 increases cell growth and survival in various cell lines. Transfection of Y-1 adrenocortical tumor cells with an IGFBP-2 expression vector resulted in a highly malignant phenotype with enhanced cellular proliferation (41). Overexpression of IGFBP-2 in human prostate cancer LNCaP cells induced a hormone-resistant and chemoresistant phenotype (40). Likewise, Miyake et al. showed that overexpression of IGFBP-2 in KoTCC-1 cells, a bladder cancer line that produces little endogenous IGFBP-2, enhanced the metastatic potential of these cells (42). SNB19 glioma cells transfected with IGFBP-2-expressing vector resulted in cells with increased cellular invasion and migration based on *in vitro* assays (43).

Overexpression of IGFBP-2 in the MDA-MB-231 cell line increased growth rates *in vitro* and *in vivo*. Significant differences in cell growth and viability between MDA-MB-231BP-2 and MDA-MB-231Mock controls when grown in serum-starved conditions emerged after day 6 of *in vitro* culture. Prior work showed that IGFBP-2-transfected Y-1 adrenocortical cancer cells exhibit their greatest growth advantage between days 4 and 6 (44). These results suggest that accumulation of a threshold concentration of IGFBP-2 may be required before the mitogenic and cytoprotective effects of IGFBP-2 are observed. Overexpression of IGFBP-2 also increases chemoresistance in MDA-MB-231 cells both *in vitro* and *in vivo*. Surprisingly, IGFBP-2-overexpressing cells treated with OGX-225 were more chemosensitive than Mock-lentivirus-infected cells. Furthermore, MDA-MB-231BP-2 cells exhibited increased rates of apoptosis after OGX-225 treatment compared with MDA-MB-231Mock cells. These results suggest that IGFBP-2-overexpressing cells become reliant on IGFBP-2-dependent pathways for cellular proliferation.

MDA-MB-468 breast cancer cells, which endogenously produce high levels of IGFBP-2, also responded to OGX-225-induced IGFBP-2 knockdown in a dose-dependent and sequence-specific manner. OGX-225 reduced IGFBP-2 expression to levels undetectable by Western blotting in MDA-MB-468 cells, and this was associated with reduced cell proliferation and increased apoptotic rates. We reported similar effects with down-regulation of IGFBP-2 in androgen-responsive LNCaP prostate cancer cells, where IGFBP-2 knockdown increased LNCaP cell apoptosis rates *in vitro* and suppressed castrate-resistant xenograft growth (40). The mechanism by

which IGFBP-2 stimulates proliferation in our systems is currently under investigation to determine if these effects can be attributed to increased IGF-I receptor activation, IGF-I receptor-independent growth effects, or both.

Clinical studies showing the efficacy of trastuzumab, a humanized monoclonal antibody to HER-2, in patients with breast cancers that overexpress HER-2 illustrate that therapy targeting deranged signaling pathways can delay progression in breast cancer (45, 46). There is a clear need to extend this paradigm to additional molecular targets, especially considering that HER-2 overexpression occurs in <20% of breast cancers (47). Our TMA analysis shows that high proportion of breast cancers express IGFBP-2, raising the possibility that a large subset of breast cancer patients may benefit from IGFBP-2-targeted therapy.

Recently, studies have shown IGFBP-2 expression may be regulated through the PI3K/Akt/mammalian target of rapamycin signaling pathway (13, 14, 35). Using the MCF-7 breast cancer cell line, Martin et al. showed that inhibition of the PI3K signaling pathway using LY294002 or the mammalian target of rapamycin inhibitor rapamycin, IGFBP-2 expression was markedly reduced; conversely, activation of PI3K signaling increased IGFBP-2 levels (35). Interestingly, IGFBP-2 may regulate PTEN, a key negative regulator in PI3K signaling pathway, in MCF-7 cells (14). Levitt et al. showed that overexpression of PTEN in the PTEN-null glioma cell line U241 reduced IGFBP-2 expression at the mRNA and protein levels (13). Combined, these results suggest that IGFBP-2 plays an important role in PI3K signaling, and the suppression of IGFBP-2 may also have selective anticancer activity in PTEN-null cancers, which has been shown to be important in breast cancer progression (48) and sensitivity to cytotoxic, hormonal, and HER2 targeting treatments (49, 50).

In summary, our results show that IGFBP-2 expression is more highly expressed in breast cancer than benign tissue and showed a strong trend to adverse survival in hormone receptor-negative invasive breast cancer. Overexpression of IGFBP-2 in the MDA-MB-231 ER-negative breast cancer cell line conferred a growth advantage and chemoresistance. Correspondingly, down-regulation of IGFBP-2 using OGX-225, both in IGFBP-2-overexpressing MDA-MB-231BP-2 cells and in MDA-MB-468 cells that endogenously produces IGFBP-2, abrogates the cytoprotective benefits of IGFBP-2. Combined, these results contribute to the rationale for evaluating OGX-225 as a candidate therapeutic for IGFBP-2-expressing breast cancers.

Disclosure of Potential Conflicts of Interest

M. Gleave is employed by OncoGenex Technologies and has an ownership interest in the company.

References

- Pollak MN, Schernhammer ES, Hankinson SE. Insulin-like growth factors and neoplasia. *Nat Rev Cancer* 2004;4:505–18.
- Firth SM, Baxter RC. Cellular actions of the insulin-like growth factor binding proteins. *Endocr Rev* 2002;23:824–54.
- Wetterau LA, Moore MG, Lee KW, Shim ML, Cohen P. Novel aspects of the insulin-like growth factor binding proteins. *Mol Genet Metab* 1999;68:161–81.
- el Atiq F, Garrouste F, Remacle-Bonnet M, Sastre B, Pommier G. Alterations in serum levels of insulin-like growth factors and insulin-like growth-factor-binding proteins in patients with colorectal cancer. *Int J Cancer* 1994;57:491–7.
- Karasik A, Menczer J, Pariente C, Kanety H. Insulin-like growth factor-1 (IGF-I) and IGF-binding protein-2 are increased in cyst fluids of epithelial ovarian cancer. *J Clin Endocrinol Metab* 1994;78:271–6.
- Lee DY, Kim SJ, Lee YC. Serum insulin-like growth factor (IGF)-I and IGF-binding proteins in lung cancer patients. *J Korean Med Sci* 1999;14:401–4.
- Cohen P, Peehl DM, Stamey TA, Wilson KF, Clemmons DR, Rosenfeld RG. Elevated levels of insulin-like growth factor-binding protein-2 in the serum of prostate cancer patients. *J Clin Endocrinol Metab* 1993;76:1031–5.
- Mishra L, Bass B, Ooi BS, Sidawy A, Korman L. Role

- of insulin-like growth factor-I (IGF-I) receptor, IGF-I, and IGF binding protein-2 in human colorectal cancers. *Growth Horm IGF Res* 1998;8:473–9.
9. Bouille N, Logie A, Gicquel C, Perin L, Le Bouc Y. Increased levels of insulin-like growth factor II (IGF-II) and IGF-binding protein-2 are associated with malignancy in sporadic adrenocortical tumors. *J Clin Endocrinol Metab* 1998;83:1713–20.
 10. McGuire SE, Hilsenbeck SG, Figueroa JA, Jackson JG, Yee D. Detection of insulin-like growth factor binding proteins (IGFBPs) by ligand blotting in breast cancer tissues. *Cancer Lett* 1994;77:25–32.
 11. Pekonen F, Nyman T, Ilvesmaki V, Partanen S. Insulin-like growth factor binding proteins in human breast cancer tissue. *Cancer Res* 1992;52:5204–7.
 12. Korc-Grodzicki B, Ren N, Hilf R. Effects of estradiol on the expression and production of IGFBP-2 by R3230AC mammary tumor cells. *Oncol Res* 1996;8:473–83.
 13. Levitt RJ, Georgescu MM, Pollak M. PTEN-induction in U251 glioma cells decreases the expression of insulin-like growth factor binding protein-2. *Biochem Biophys Res Commun* 2005;336:1056–61.
 14. Perks CM, Vernon EG, Rosendahl AH, Tonge D, Holly JM. IGF-II and IGFBP-2 differentially regulate PTEN in human breast cancer cells. *Oncogene* 2007;26:5966–72.
 15. American Cancer Society. *Cancer facts and figures 2005*. Atlanta: American Cancer Society, Inc.; 2005. p. 9–11.
 16. Osteen R. *The American Cancer Society's clinical oncology*. Atlanta: American Cancer Society, Inc.; 2001. p. 251–68.
 17. Chi KN, Eisenhauer E, Fazli L, et al. A phase I pharmacokinetic and pharmacodynamic study of OGX-011, a 2'-methoxyethyl antisense oligonucleotide to clusterin, in patients with localized prostate cancer. *J Natl Cancer Inst* 2005;97:1287–96.
 18. Leung S, Miyake H, Zellweger T, Tolcher A, Gleave ME. Synergistic chemosensitization and inhibition of progression to androgen independence by antisense Bcl-2 oligodeoxynucleotide and paclitaxel in the LNCaP prostate tumor model. *Int J Cancer* 2001;91:846–50.
 19. Miyake H, Eto H, Hara I, So A, Li D, Gleave ME. Synergistic antitumor activity by combined treatment with gemcitabine and antisense oligodeoxynucleotide targeting clusterin gene in an intravesical administration model against human bladder cancer KoTCC-1 cells. *J Urol* 2004;171:2477–81.
 20. Cheang MC, Treaba DO, Speers CH, et al. Immunohistochemical detection using the new rabbit monoclonal antibody SP1 of estrogen receptor in breast cancer is superior to mouse monoclonal antibody 1D5 in predicting survival. *J Clin Oncol* 2006;24:5637–44.
 21. Lohrisch C, Jackson J, Jones A, Mates D, Olivotto IA. Relationship between tumor location and relapse in 6,781 women with early invasive breast cancer. *J Clin Oncol* 2000;18:2828–35.
 22. Chia SK, Speers CH, Bryce CJ, Hayes MM, Olivotto IA. Ten-year outcomes in a population-based cohort of node-negative, lymphatic, and vascular invasion-negative early breast cancers without adjuvant systemic therapies. *J Clin Oncol* 2004;22:1630–7.
 23. Cheang MC, Voduc D, Bajdik C, et al. Basal-like breast cancer defined by five biomarkers has superior prognostic value than triple-negative phenotype. *Clin Cancer Res* 2008;14:1368–76.
 24. Yu D, Chen D, Chiu C, Razmazma B, Chow YH, Pang S. Prostate-specific targeting using PSA promoter-based lentiviral vectors. *Cancer Gene Ther* 2001;8:628–35.
 25. Monia BP, Lesnik EA, Gonzalez C, et al. Evaluation of 2'-modified oligonucleotides containing 2'-deoxy gaps as antisense inhibitors of gene expression. *J Biol Chem* 1993;268:14514–22.
 26. Rocchi P, So A, Kojima S, et al. Heat shock protein 27 increases after androgen ablation and plays a cytoprotective role in hormone-refractory prostate cancer. *Cancer Res* 2004;64:6595–602.
 27. Gleave ME, Hsieh JT, Wu HC, von Eschenbach AC, Chung LW. Serum prostate specific antigen levels in mice bearing human prostate LNCaP tumors are determined by tumor volume and endocrine and growth factors. *Cancer Res* 1992;52:1598–605.
 28. Gebauer G, Jager W, Lang N. mRNA expression of components of the insulin-like growth factor system in breast cancer cell lines, tissues, and metastatic breast cancer cells. *Anticancer Res* 1998;18:1191–5.
 29. Busund LT, Richardson E, Busund R, et al. Significant expression of IGFBP2 in breast cancer compared with benign lesions. *J Clin Pathol* 2005;58:361–6.
 30. Fukushima T, Tezuka T, Shimomura T, Nakano S, Kataoka H. Silencing of insulin-like growth factor-binding protein-2 in human glioblastoma cells reduces both invasiveness and expression of progression-associated gene CD24. *J Biol Chem* 2007;282:18634–44.
 31. Miyake H, Hara I, Yamanaka K, Muramaki M, Eto H. Prognostic significance of insulin-like growth factor (IGF) binding protein-2 to IGF-binding protein-3 ratio in patients undergoing radical cystectomy for invasive transitional cell carcinoma of the bladder. *BJU Int* 2005;95:987–91.
 32. Vorwerk P, Wex H, Hohmann B, Mohnike K, Schmidt U, Mittler U. Expression of components of the IGF signalling system in childhood acute lymphoblastic leukaemia. *Mol Pathol* 2002;55:40–5.
 33. Inman BA, Harel F, Audet JF, et al. Insulin-like growth factor binding protein 2: an androgen-dependent predictor of prostate cancer survival. *Eur Urol* 2005;47:695–702.
 34. Clemmons DR, Camacho-Hubner C, Coronado E, Osborne CK. Insulin-like growth factor binding protein secretion by breast carcinoma cell lines: correlation with estrogen receptor status. *Endocrinology* 1990;127:2679–86.
 35. Martin JL, Baxter RC. Expression of insulin-like growth factor binding protein-2 by MCF-7 breast cancer cells is regulated through the phosphatidylinositol 3-kinase/AKT/mammalian target of rapamycin pathway. *Endocrinology* 2007;148:2532–41.
 36. Fog CK, Christensen IJ, Lykkesfeldt AE. Characterization of a human breast cancer cell line, MCF-7/RU58R-1, resistant to the pure antiestrogen RU 58,668. *Breast Cancer Res Treat* 2005;91:133–44.
 37. Helle SI, Mietlowski W, Guastalla JP, et al. Effects of tamoxifen and octreotide LAR on the IGF-system compared with tamoxifen monotherapy. *Eur J Cancer* 2005;41:694–701.
 38. Gronbaek H, Flyvbjerg A, Mellemejaer L, et al. Serum insulin-like growth factors, insulin-like growth factor binding proteins, and breast cancer risk in postmenopausal women. *Cancer Epidemiol Biomarkers Prev* 2004;13:1759–64.
 39. Nickerson T, Miyake H, Gleave ME, Pollak M. Castration-induced apoptosis of androgen-dependent Shionogi carcinoma is associated with increased expression of genes encoding insulin-like growth factor-binding proteins. *Cancer Res* 1999;59:3392–5.
 40. Kiyama S, Morrison K, Zellweger T, et al. Castration-induced increases in insulin-like growth factor-binding protein 2 promotes proliferation of androgen-independent human prostate LNCaP tumors. *Cancer Res* 2003;63:3575–84.
 41. Hoefflich A, Fettscher O, Lahm H, et al. Overexpression of insulin-like growth factor-binding protein-2 results in increased tumorigenic potential in Y-1 adrenocortical tumor cells. *Cancer Res* 2000;60:834–8.
 42. Miyake H, Hara I, Yamanaka K, Muramaki M, Gleave M, Eto H. Introduction of insulin-like growth factor binding protein-2 gene into human bladder cancer cells enhances their metastatic potential. *Oncol Rep* 2005;13:341–5.
 43. Wang H, Shen W, Huang H, et al. Insulin-like growth factor binding protein 2 enhances glioblastoma invasion by activating invasion-enhancing genes. *Cancer Res* 2003;63:4315–21.
 44. Hoefflich A, Fettscher O, Preta G, et al. Increased activity of catalase in tumor cells overexpressing IGFBP-2. *Horm Metab Res* 2003;35:816–21.
 45. Romond EH, Perez EA, Bryant J, et al. Trastuzumab plus adjuvant chemotherapy for operable HER2-positive breast cancer. *N Engl J Med* 2005;353:1673–84.
 46. Papaldo P, Fabi A, Ferretti G, et al. A phase II study on metastatic breast cancer patients treated with weekly vinorelbine with or without trastuzumab according to HER2 expression: changing the natural history of HER2-positive disease. *Ann Oncol* 2006;17:630–6.
 47. Wolff AC, Hammond ME, Schwartz JN, et al. American Society of Clinical Oncology/College of American Pathologists guideline recommendations for human epidermal growth factor receptor 2 testing in breast cancer. *Arch Pathol Lab Med* 2007;131:18.
 48. Dupont J, Renou JP, Shani M, Hennighausen L, LeRoith D. PTEN overexpression suppresses proliferation and differentiation and enhances apoptosis of the mouse mammary epithelium. *J Clin Invest* 2002;110:815–25.
 49. Clark AS, West K, Streicher S, Dennis PA. Constitutive and inducible Akt activity promotes resistance to chemotherapy, trastuzumab, or tamoxifen in breast cancer cells. *Mol Cancer Ther* 2002;1:707–17.
 50. Nagata Y, Lan KH, Zhou X, et al. PTEN activation contributes to tumor inhibition by trastuzumab, and loss of PTEN predicts trastuzumab resistance in patients. *Cancer Cell* 2004;6:117–27.